



# Chest Tuberculosis in Children

Priyanka Naranje<sup>1</sup> · Ashu Seith Bhalla<sup>1</sup> · Poonam Sherwani<sup>1</sup>

Received: 8 October 2018 / Accepted: 20 December 2018 / Published online: 14 February 2019  
© Dr. K C Chaudhuri Foundation 2019

## Abstract

Chest is the commonest site of involvement by tuberculosis (TB) in children; lungs being the most frequently affected region, followed by nodes, pleura and chest wall. It is difficult to diagnose TB in children due to lack of overt symptoms and difficulty in obtaining samples for microbiological confirmation. Hence various imaging modalities play an important role in diagnostic algorithm as well as in follow-up after treatment. Standardization of chest radiograph reporting in context of clinically suspected TB is the need of the hour so as to suggest a proper diagnosis and avoid over-diagnosis. This article aims to discuss the imaging features of chest tuberculosis according to the site of involvement on various imaging modalities in the pediatric population.

**Keywords** Chest tuberculosis · Children · Imaging · Recommendations · CT · Ultrasound · MRI

## Introduction

Imaging is an important cornerstone of diagnosis of chest tuberculosis (CTB) in children. This is because tuberculosis (TB) in children is often paucibacillary, and obtaining microbiological confirmation is challenging. Thoracic TB includes pulmonary TB (PTB) as well as extrapulmonary TB (EPTB). EPTB sites in the chest being nodes, pleura and chest wall. Imaging appearances of CTB have classically been divided as primary disease, progressive primary disease and post-primary (or reactivation or adult type) patterns. This distinction being based on the time related course of the disease. However, several studies have shown an overlap in the features of these forms. Also, recent studies have illustrated, based on epidemiological and genetic studies, that it is the immunity of the host, rather than time since exposure that governs the pattern [1]. In this article, hence, authors discuss the imaging features according to the site of involvement on various imaging modalities, rather than primary or post-primary disease.

## Role of Imaging

Imaging is not only important for diagnosis, but equally critical for follow-up and response assessment. In addition, after the active infection heals, children may present with symptoms attributable to sequelae of infection. These symptoms may appear in childhood or even years later in adulthood. The presentations include dyspnea, hemoptysis or cough with expectoration. These clinical presentations may suggest reactivation of TB, but can also occur as a consequence of fibrotic sequelae (with /without secondary bacterial infection or fungal colonization); without any active TB. This distinction is critical in order to avoid unnecessary administration of antitubercular treatment (ATT). The basis of this distinction again rests on imaging, in addition to microbiology. Imaging has to achieve all these goals while keeping the radiation and economic burden to the patient to a minimum.

## Imaging Modalities

### Chest Radiograph

Chest radiograph (CXR) remains the primary imaging modality for evaluation of a child suspected of thoracic tuberculosis. CXR, however, suffers from lower sensitivity of 67% [2] (relative to cross-sectional imaging techniques CT/MR); and also from considerable interobserver variability [3]. The radiographic appearance of CTB is discussed below.

---

✉ Ashu Seith Bhalla  
ashubhalla1@yahoo.com

<sup>1</sup> Department of Radiodiagnosis, All India Institute of Medical Sciences, New Delhi 110029, India

**Table 1** Signs of lymphadenopathy on frontal chest radiograph

Right hilar adenopathy	<ul style="list-style-type: none"> <li>• Obliteration of hilar point (normally outwardly pointing ‘U’)</li> <li>• Increased density of hilum</li> <li>• Lobulated outline</li> <li>• Compression of bronchus intermedius (When associated subcarinal lymph nodes)</li> </ul>
Left hilar adenopathy	<ul style="list-style-type: none"> <li>• Less frequent</li> <li>• Signs similar to right, except left hilar nodes are detected when larger <i>i.e.</i>, when these project beyond left cardiac border</li> </ul>
Right paratracheal lymphadenopathy	<ul style="list-style-type: none"> <li>• Lobulated soft tissue extending beyond thymus or cardiac border</li> <li>• Displacement/Compression of trachea (not seen with enlarged thymus, which is the main differential diagnosis)</li> </ul>
Left paratracheal lymphadenopathy	<ul style="list-style-type: none"> <li>• Often associated with right paratracheal adenopathy</li> <li>• Inferior displacement/compression of left main bronchus (not seen with enlarged thymus)</li> </ul>
Airway compression	<ul style="list-style-type: none"> <li>• More in infants than older children</li> <li>• More in multifocal disease</li> <li>• Site of compression correlation with nodal group enlarged Trachea – Paratracheal nodes Left main bronchus – Left hilar nodes Right bronchus intermedius – Right hilar with subcarinal nodes</li> </ul>

## Lymphadenopathy

Identification of lymphadenopathy is an important, and often the only radiographic manifestation of the primary TB. Several signs have been described on CXR for more objective diagnosis of hilar/mediastinal adenopathy, and Table 1 describes these signs (Figs. 1 and 2).

Lateral CXR is superior to frontal CXR for the diagnosis of subcarinal nodes. Hence while in some centres lateral CXRs are not routinely used, these can be a useful adjunct when lymphadenopathy is suspected on frontal CXR. Subcarinal/retrocarinal nodes appear as oval/round soft tissue densities posterior/inferior to bronchus intermedius (Doughnut sign).

## Lung Parenchymal Changes

Primary TB tends to involve the middle and lower lobes of right lung more than left lung. CXR reveals areas of increased opacity in the form of consolidation (focal or multilobar) or nodules clustered in one zone or miliary (distributed diffusely). Consolidation may show cavitation.

## Pleural/ Chest Wall Involvement

In addition, presence of pleural effusion and bone (rib/vertebral) destruction may be identified on CXR. Tubercular pleural effusion is typically “free” pleural effusion with a rising fluid level. The presence of

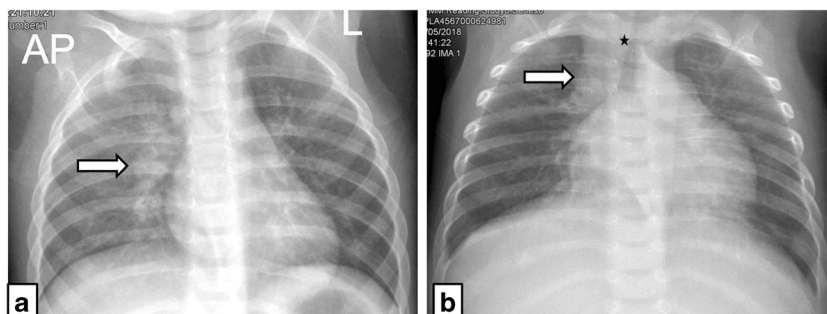
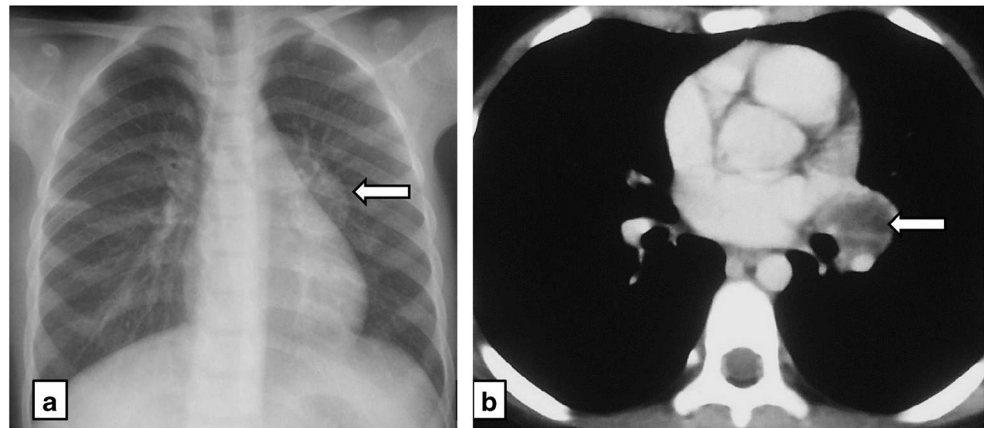


**Fig. 1** Right hilar and paratracheal lymphadenopathy. **a** Chest radiograph of a 1-y-old girl shows enlarged right hilar lymph nodes (*arrow*) with convex outline and loss of normal concave hilum. **b** A 7-mo-old child presented with fever and hepatosplenomegaly. Chest radiograph shows

lobulated right paratracheal lymph node (*arrow*) extending beyond the margin of thymus. In addition, compression on the trachea is also noted (*asterisk*)

**Fig. 2** Left hilar lymphadenopathy. **a** Chest radiograph of a child with low grade fever and cough shows lobulated soft tissue in left parahilar region extending beyond the left heart border s/o left hilar lymph nodes (*arrow*). **b** CECT chest of the same child shows necrotic, rim enhancing left hilar lymph nodes (*arrow*)



loculations, as evidenced by convex medial border of effusion, along with volume loss is suggestive of empyema formation.

### Standardization of CXR Report

Several standardized approaches to report the chest radiograph have been proposed, but not yet universally accepted. The authors recommend the use of following terminology (Table 2) (Figs. 3, 4, 5) [4–6].

**Probable:** The term ‘probable’ is suggested when CXR findings are non-specific but can be consistent with TB (*e.g.*,

consolidation, infiltrates or nodules) with presence of one of the following: documented exposure, tuberculin skin sensitivity (TST) positive or response to ATT.

**Possible:** The term ‘possible’ is suggested when CXR findings are similar to the probable category but there is no documented exposure, no response to ATT and TST is negative. If CXR findings are inconsistent with TB, however, atleast one of the following features is present: documented exposure, TST positive or response to ATT; then also it is a possible TB [7].

### Response Assessment

CXR is valuable in monitoring the response to treatment, as well as detecting complications. To the best of authors’ knowledge, there are no guidelines available for the need or frequency of follow-up CXRs. The authors recommend to repeat the CXR at the end of intensive phase (IP) of treatment for patients showing persistent symptoms or slow resolution of symptoms. CXR at the end of IP is not required for patients who are improving but it should be performed at the end of continuation phase in all to document response. The importance of a CXR performed on the completion of therapy is also that it serves as baseline imaging, in case the patient subsequently presents with respiratory symptoms. Comparison with this CXR aids in the distinction between reactivation of TB vs. symptomatic sequelae.

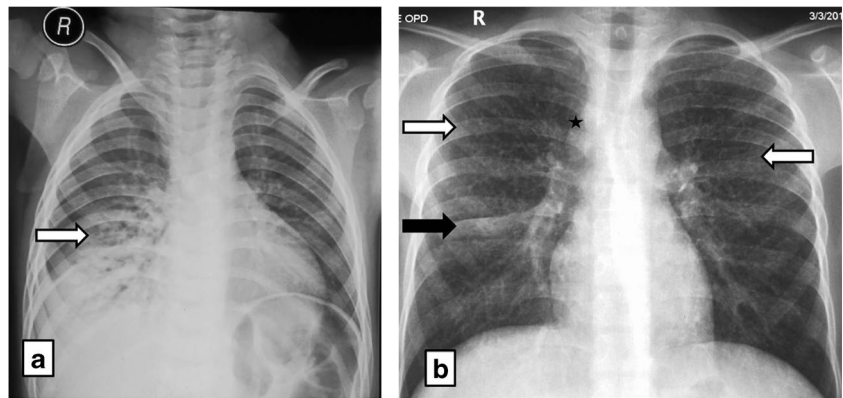
### Ultrasonography

Ultrasonography (USG) evaluation of the lung is one of the newer applications of USG, and it has gained utmost importance especially in critical care. Thin chest wall and non-calcified costal cartilages; besides being a

**Table 2** Recommendations of CXR reporting terminology in a suspected case of TB

A. Highly Suggestive CXR findings for TB
• Hilar / paratracheal lymphadenopathy with or without parenchymal lesions
• Miliary nodules
• Consolidation with cavitation/Fibrosis
B. Suggestive but nonspecific CXR findings for TB (Probable/Possible)
• Equivocal hilar/ paratracheal stripe enlargement
• Consolidation
• Thin walled cavities
• Indeterminate/airspace nodules
C. Alternate diagnosis
• CXR may reveal features consistent or suggestive of an alternate etiology or be normal.
D. Healed TB/ Sequelae of TB
• Thin-walled cavity
• Bronchiectasis
• Fibroparenchymal/reticular opacities
• Atelectasis/collapse
• Calcified mediastinal lymph nodes
• Pleural thickening/calcification

**Fig. 3** CXR findings ‘Highly suggestive of TB’. **a** Radiograph showing consolidation of right mid and lower zones (*arrow*) with areas of cavitation. **b** Another child with history of fever and weight loss shows multiple miliary nodules (*white arrows*) in bilateral lung fields, consolidation in right mid zone (*black arrow*), enlarged nodes in right paratracheal region (*asterisk*)



cheaper, radiation free modality; makes USG a suitable technique for evaluation of nodes, pleura and even lung parenchyma in children. The addition of USG to CXR, enhances the diagnostic confidence, and may obviate the need for a CT chest in several children.

**Mediastinal Nodes**

Recently, the utility of USG in the evaluation of mediastinal nodes has been demonstrated [8]. In some studies it has shown to be more sensitive (upto 67%) compared with CXR for identification of mediastinal lymph nodes [9]. Any basic USG machine with availability of linear, convex/microconvex and endocavitary probes can be used. For visualisation of right and left paratracheal nodes, linear probe can be used over parasternal regions. Suprasternal approach using an endocavitary probe can also be used. For the prevascular and subcarinal nodes,

microconvex probe is most appropriate. Lower mediastinal and posterior mediastinal nodes are usually not visualised using ultrasound. Apart from chest, a quick screening USG of abdomen may reveal periportal and other lymph nodes, liver and splenic granulomas which may help corroborating the diagnosis of TB. Nodes appear hypoechoic, round to oval lesions, seen adjacent to mediastinal vessels (Fig. 6a). These may show hyperechoic foci of calcifications or even internal anechoic areas at times. The anechoic areas represent necrosis. USG for mediastinal lymph nodes is limited by operator dependence and a relatively long learning curve.

**Pleural Collections**

USG has long being utilised for evaluation of pleural fluid collections for both identification, quantification as well as for guided drainages. USG helps detecting the anechoic

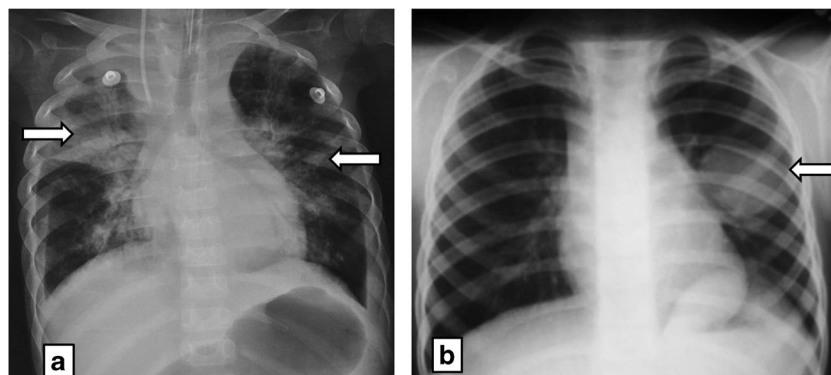
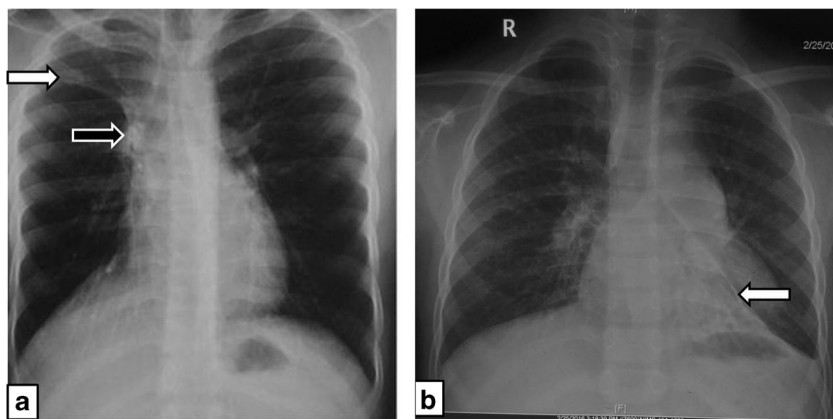


**Fig. 4** CXR findings ‘Probable/possible TB’ and ‘alternate diagnosis’. **a** CXR findings of ‘Probable/possible TB’. Frontal radiograph shows multifocal areas of consolidation in both lungs (*arrows*) with bilateral pleural effusion. **b** CXR findings of ‘Alternate diagnosis’. Radiograph

of an 11- y- old child with history of cough. CXR shows well margined mass lesion in left midzone (*arrow*). No consolidation, lymphadenopathy, or effusion seen

**Fig. 5** CXR findings of healed TB. **a** Frontal radiograph of a 14-y- child with past history of tuberculosis shows fibrotic opacities in right upper zone (*white arrow*) with pulled up right hilum and calcified right hilar lymph nodes (*black arrow*). **b** Radiograph of an 11-y-old child post antituberculous treatment shows left lower lobe collapse with fibrobronchiectatic changes (*arrow*)



fluid in pleural cavity without any pleural thickening or septations which represent free effusion; or it may show the multiple echoes, septations and loculations with pleural thickening in empyema (Fig. 6b). It is hence invaluable in taking a decision regarding drainage.

### Parenchymal Lesions

In addition to nodes and pleura, a systematic zone wise assessment of the entire chest can be done for evaluation of lung parenchyma, for those areas of consolidation or

**Fig. 6** Ultrasound findings of chest tuberculosis in different patients. **a** Transverse ultrasound image through parasternal approach shows large necrotic lymph node in the prevascular region anterior to superior vena cava (SVC) (*arrow*). **b** USG using linear transducer shows septated pleural collection (*arrow*) with presence of pleural thickening. **c** Left mid zone USG using curvilinear transducer through intercostal approach shows discontinuation of pleural line with irregular shredded appearance of margins of the consolidation suggestive of 'shred sign' (*arrow*). **d** Large area of consolidation with air bronchogram (*arrow*)

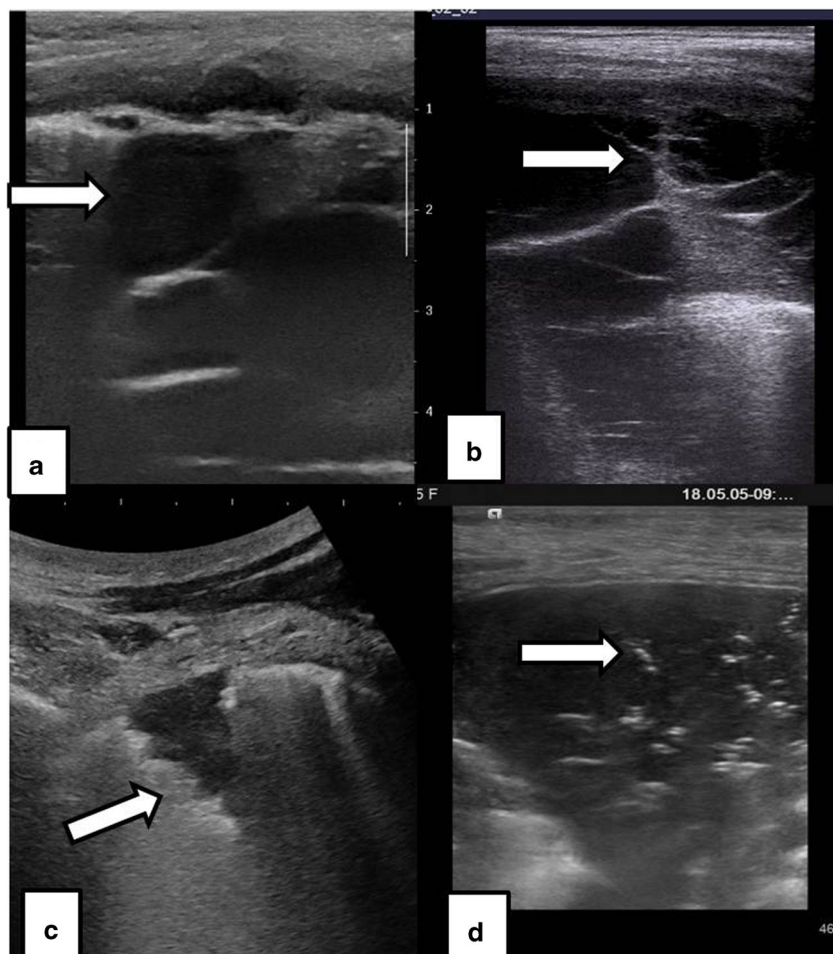


**Table 3** CT features of active vs. healed nodes of TB

Active Disease	Changes with Healing
Enlargement	Decrease in size
Central necrosis with rim enhancement	Homogeneous
Heterogeneous /ghost like enhancement Homogenous*	Homogeneous
Obscured perinodal fat	Appearance of perinodal fat
Coalescence	Discrete nodes seen
Calcification (28.4% [11])	Calcification (41.7% increase in size and density [11])

\*Active nodes may not show necrosis and appear homogeneous [12]

large nodules which abut the pleural margin. USG can show these regions as hypochoic areas with or without air bronchograms. Various signs are also described for identifying lung abnormalities of consolidation/collapse on USG. These include, “shred sign” (Fig. 6c), “tissue-like sign”, “static or dynamic air bronchogram sign” (Fig. 6d) and “loss of curtain sign”. USG can also detect complications such as areas of cavitation or formation of lung abscess within the areas of consolidation.

### Computed Tomography

Despite radiation concerns, computed tomography (CT) continues to maintain its dominance as the preferred cross-sectional imaging modality in the evaluation of complex thoracic disorders in both children and adults. This is due to capability of CT to complete imaging the entire thorax in a single breathhold, with significant dose reductions achieved by vendors over the years.

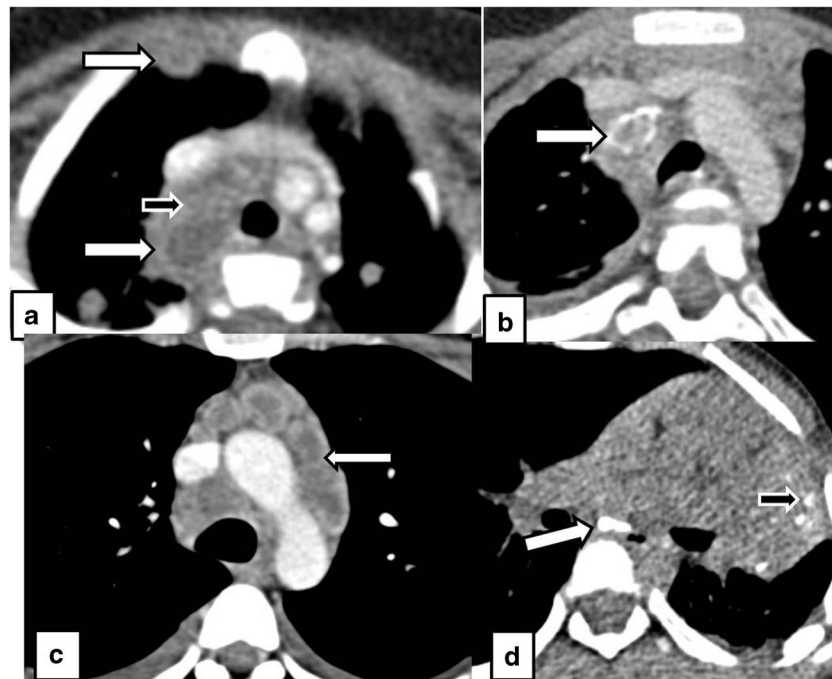


**Fig. 7** Lymphadenopathy on CT (different patients). **a** Contrast enhanced axial CT of a 1-y-old child shows enlarged peripherally enhancing necrotic lymph nodes in right paratracheal and right internal mammary locations (*white arrows*) with perinodal fat stranding (*black arrow*) s/o active tuberculosis. **b** CECT of a child on antituberculous therapy shows partially calcified right paratracheal lymph node (*arrow*) along with other

non-calcified nodes in prevascular locations and right pleural effusion. **c** CECT axial scan at the level of aortic arch shows multiple enlarged ‘conglomerate’ necrotic lymph nodes in prevascular and pretracheal location. **d** Low dose NCCT of child on ATT shows calcified subcarinal lymph node (*arrow*) with parenchymal calcifications in a collapsed left upper lobe (*black arrow*)

**Table 4** CT features of various lung parenchymal findings

Type of morphological abnormality	Special features
Consolidation	Homogeneous or with internal necrosis
Cavities	Often multifocal Within an area of consolidation or separate Thick walled with or without air-fluid levels
Nodules	<ul style="list-style-type: none"> <li>• Centrilobular nodules due to bronchial impaction with mucoid/inflammatory exudates</li> <li>• Localized, asymmetric, in distribution of a bronchus, giving the classical ‘tree-in-bud’ opacities</li> <li>• Random nodules are seen as miliary nodules of 1-3 mm size</li> <li>• Larger, fewer nodules with or without cavitations</li> <li>• Perilymphatic nodules are classical of sarcoidosis but have been reported in TB also recently. However, this is an infrequent finding.</li> <li>• ‘Halo’ and ‘reverse halo’ signs are also infrequent patterns reported in TB; although these are classical for invasive pulmonary aspergillosis and organising pneumonia respectively.</li> </ul>
Tuberculoma	Refers to well defined nodule measuring upto 1–5 cm [14]
Atelectasis/ air trapping	Maybe seen distal to site of airway compression/erosion by lymph nodes.

### Indications for CECT Chest

1. Equivocal/normal CXR (strong clinical suspicion but no alternative diagnosis established)
2. Severe /complicated infections
3. Immunocompromised host
4. Preprocedure evaluation

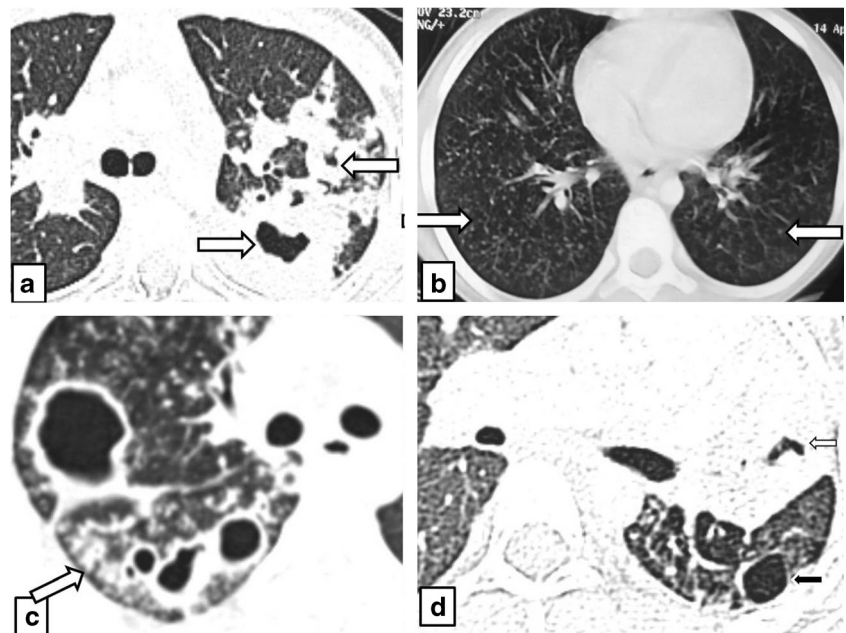
It is prudent to use CT prior to immune suppression in patients with equivocal radiographs. The differentiation of

latent from active TB can be challenging on a CXR, and CT has a higher diagnostic accuracy in this regard too [10].

The initial CT of a patient should be contrast-enhanced, unless there is a contraindication to the use of contrast. This allows for a comprehensive evaluation of the extent and involved sites of the infection. On follow-up, if only parenchymal changes need to be assessed NCCT with HRCT reconstruction will suffice.

The imaging findings assessed on CT include all the anatomic compartments of the thorax.

**Fig. 8** Lung parenchymal findings on CT. **a** CT chest of a 9-y-old child with active TB. Lung window shows multiple areas of consolidation and cavities in left lung. **b** Multiple diffuse tiny random nodules are seen in bilateral lung parenchyma in a 10-y-old child with miliary TB. **c** Multiple centrilobular nodules in right lower lobe with branching depicting classical ‘tree-in-bud’ appearance. **d** NCCT of an 8-y-old child. Lung window shows volume loss with complete collapse-consolidation of left upper lobe with fibrotic changes and thin walled cavity in left lower lobe (black arrow)



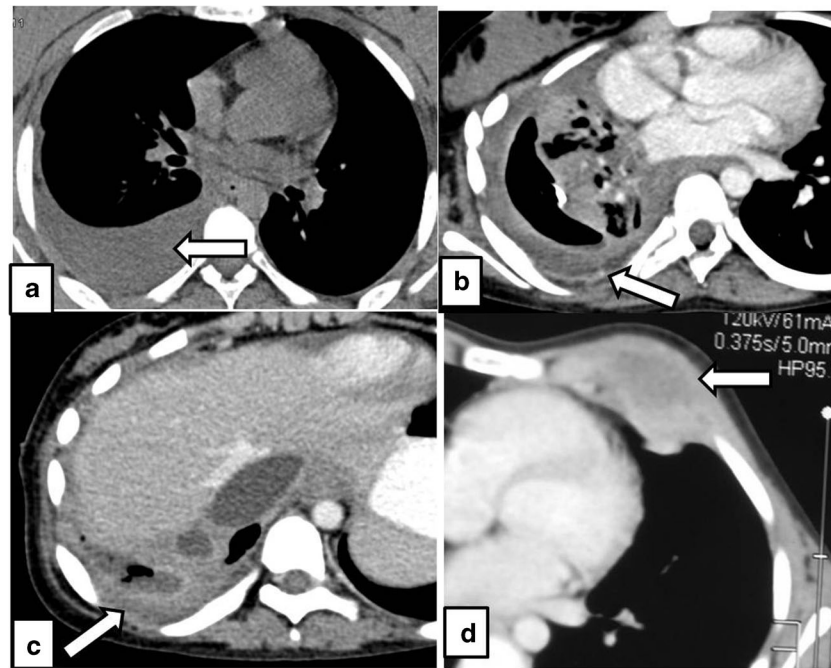


**Fig. 9** Pleural and chest wall involvement in TB. **a** NCCT of a child with fever and cough shows moderate free pleural effusion on right side (*arrow*). **b** CECT chest of a 9-y-old child with tuberculosis shows right sided empyema as suggested by enhancement of parietal pleura (*arrow*) with underlying lung consolidation-collapse and volume loss as evident by ipsilateral

crowding of ribs. **c** Inferior CT sections of same child as in **b**, shows multiple loculations and extrapleural fat proliferation and edema (*arrow*). **d** CECT chest of a 6-y-old child presenting with chest wall mass shows abscess along left anterior chest wall. The fluid was aspirated under ultrasound guidance which revealed acid-fast bacilli (AFB)

**Fig. 10** Use of MRI for follow-up. **a** CECT of child with active disease shows multiple conglomerate necrotic lymph nodes in subcarinal region (*arrow*). **b** The child was given 6 mo ATT. Follow-up MRI shows significant resolution in the lymph nodes size as well as enhancement s/o healed nodes

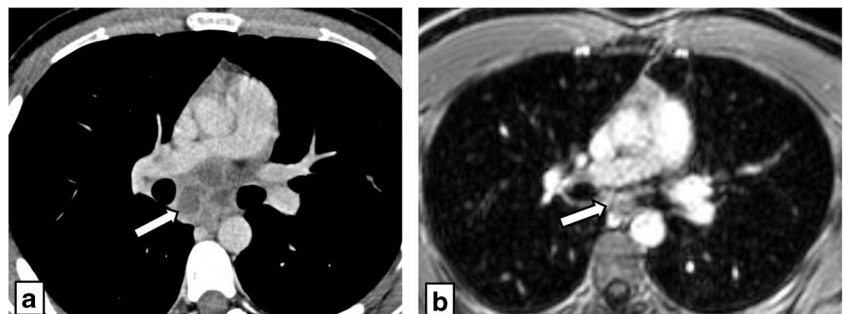


**Table 5** Appearances of nodes on various MRI sequences

MRI sequence	Signal intensity(SI) of active lymph node
T2	Hyperintense (Hypointense centre in caseous necrosis, hyperintense with more liquefaction)
T1	Iso-hypointense
Post Gadolinium	Peripheral rim enhancement Heterogeneous enhancement
DWI	Restricted diffusion

### Lymphadenopathy

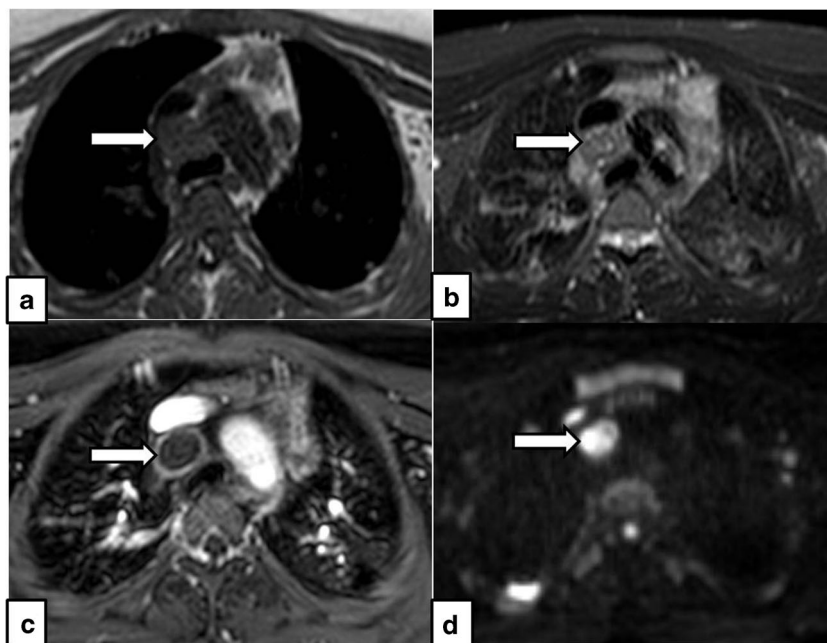
The imaging features of active and healed nodes are detailed in Table 3 [13]. Healed or fibrotic LNs may continue to appear as mildly enlarged nodes on CT, with or without calcification. (Fig. 7).

### Parenchymal Changes

Lung parenchymal findings encountered in active TB are enumerated in Table 4 (Fig. 8).



**Fig. 11** Tubercular lymphadenopathy on MRI. (a–d) MRI of a 12-y-old child with fever and sputum positive for AFB. Axial CE MRI chest revealed shows enlarged pretracheal lymph node appearing T1 hypointense (a), Intermediate signal intensity on T2W (b) and shows peripheral rim enhancement on post contrast (c) and restriction on diffusion weighted images. (Arrows from a to d)



### Pleural Involvement

Pleural effusion appears as a crescentic, free fluid collection in the pleural space with minimal or no pleural thickening (Fig. 9a) [15]. Empyema on the other hand is loculated with thick and enhancing pleura (Fig. 9b, c). Volume loss and calcification are also seen.

### Chest Wall Involvement

Common sites of chest wall involvement are the dorsal spine with pre or paravertebral abscess, sternoclavicular joint, costochondral junctions or ribs. (Fig. 9d).

### Airway Involvement

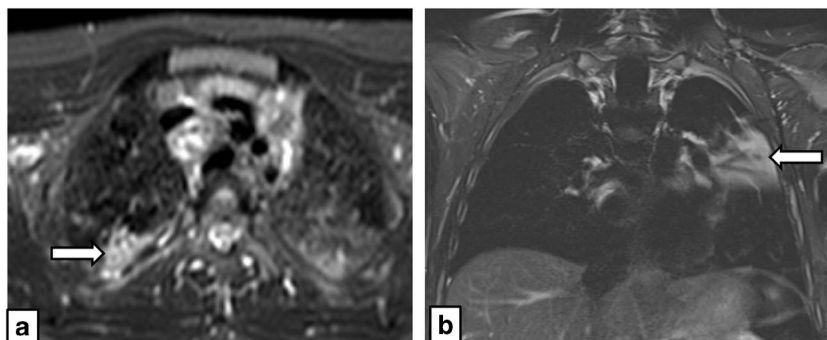
Involvement of large airways (trachea and major bronchi) can occur in active tuberculosis in the form of smooth or

irregular wall thickening, polypoidal endoluminal ulcerated mass or as peribronchial soft tissue causing extrinsic luminal narrowing of trachea or bronchi [16]. Bronchiectasis is a common sequelae of healed tuberculosis and is usually found in upper lobes as a result of destruction of lung parenchyma and fibrosis or as a result of endobronchial infection leading to damage of bronchial walls.

### Magnetic Resonance Imaging

Use of magnetic resonance imaging (MRI) in the chest has been limited by several factors including its cost and limited availability. The primary limiting factors, however, are technical. MRI has much longer acquisition times relative to CT, hence respiratory and cardiac motion cause significant image degradation. Also, poor proton density in the lungs results in poor MR signal. However, the two major advantages of MRI are its superior contrast resolution and also lack of radiation

**Fig. 12** MRI for parenchymal lesions. a MRI of a 5-y-old child with active tuberculosis. T2W image shows subpleural consolidation (arrow) with hyperintense lymph node in pretracheal region. b Coronal T2W MR image shows focal area of consolidation with air bronchogram in left upper lobe



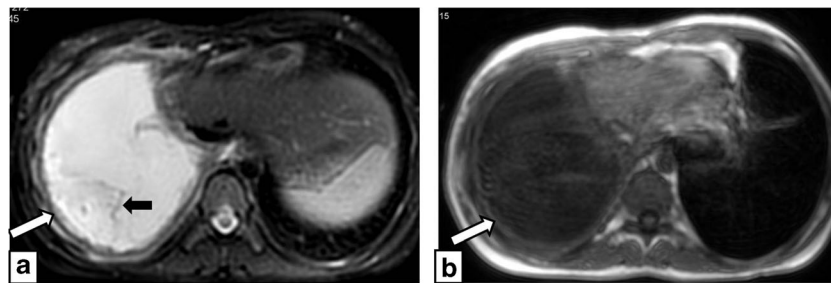


**Fig. 13** MRI for pleural fluid collections. T2 (a) and T1 (b) weighted images of a 9-y-old child with active tuberculosis shows right sided empyema appearing hyperintense on T2W and hypointense on T1W images with multiple thin septations (black arrow) and pleural thickening (white arrows)

[17]. In recent years, there have been developments which have significantly reduced imaging times, with availability of breath-hold sequences. There has understandably been an explosion of literature exploring its use in children requiring repeated imaging of the chest [18, 19].

In context of tuberculosis, its potential use is in children with drug-resistant infection requiring prolonged regimens with second line therapy. Interim, periodic assessment with MRI gives a reasonable assessment of response (Fig. 10). Also, contrast is not essential for detection and accurate size evaluation of nodes. MRI has been demonstrated to have a 100% positive predictive value for detection of nodes larger than 7 mm [20]. Contrast administration though results in better detection of necrosis. Imaging features of TB nodes are detailed in Table 5 (Fig. 11). It has also has high sensitivity for detection for pulmonary and pleural involvement (Figs. 12, 13).

### 18F FDG PET-CT

Several studies have demonstrated the utility of 18F FDG PET-CT in demonstration of active sites of tubercular involvement [21, 22]. However, the major limitation of PET-CT, besides cost and availability, is of high radiation burden. Despite newer low dose protocols, the radiation dose remains in the range of 9.6–29.8 mSv [23]. Hence PET-CT is not included in the routine diagnostic algorithm of TB in children.

### Conclusions

The authors recommend an algorithmic approach to the use of the various imaging modalities in the evaluation of pediatric tuberculosis (Fig. 14).

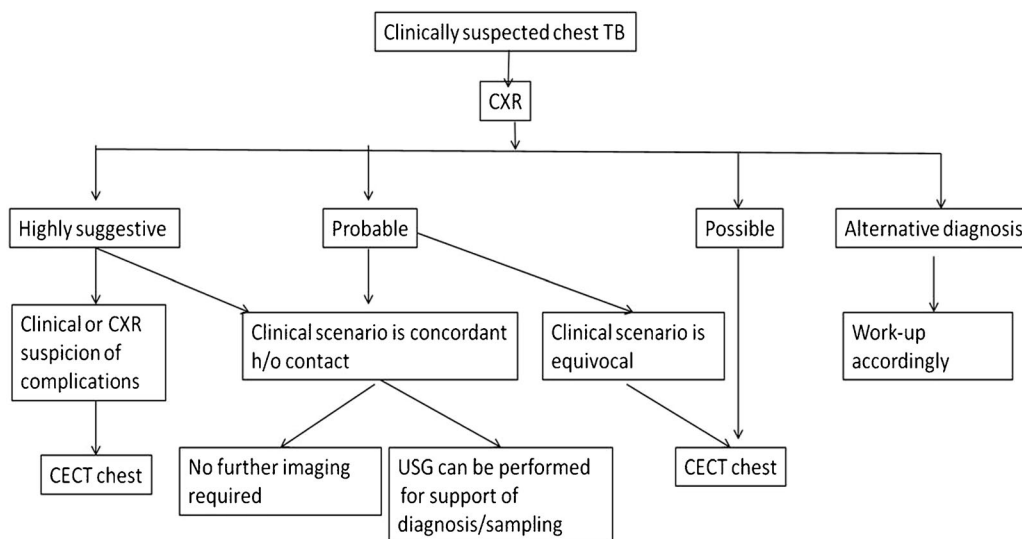


**Fig. 14** Proposed algorithm for evaluation of a child with suspected chest TB. CECT Contrast enhance CT, CXR Chest radiograph

**Author's Contribution** PN: Manuscript preparation, figures & cases and literature search; ASB: Conception and design of the work, drafting the article, critical revision of the article; PS: Literature search, writing the initial draft and figures. The final manuscript was checked and approved by all the authors. ASB will act as guarantor for this paper.

## Compliance with Ethical Standards

**Conflict of Interest** None.

**Source of Funding** None.

**Publisher's Note** Springer Nature remains neutral with regard to jurisdictional claims in published maps and institutional affiliations.

## References

1. Abel L, El-Baghdadi J, Bousfiha AA, Casanova JL, Schurr E. Human genetics of tuberculosis: a long and winding road. *Philos Trans R Soc Lond Ser B Biol Sci.* 2014;369:20130428.
2. Swingler GH, du Toit G, Andronikou S, van der Merwe L, Zar HJ. Diagnostic accuracy of chest radiography in detecting mediastinal lymphadenopathy in suspected pulmonary tuberculosis. *Arch Dis Child.* 2005;90:1153–6.
3. Du Toit G, Swingler G, Iloni K. Observer variation in detecting lymphadenopathy on chest radiography. *Int J Tuberc Lung Dis.* 2002;6:814–7.
4. Kumar A, Gupta D, Nagaraja SB, et al. Updated national guidelines for pediatric tuberculosis in India, 2012. *Indian Pediatr.* 2013;50:301–6.
5. Graham SM, Ahmed T, Amanullah F, et al. Evaluation of tuberculosis diagnostics in children: 1. Proposed clinical case definitions for classification of intrathoracic tuberculosis disease. Consensus from an expert panel. *J Infect Dis.* 2012;205:S199–208.
6. Bhalla AS, Goyal A, Guleria R, Gupta AK. Chest tuberculosis: Radiological review and imaging recommendations. *Indian J Radiol Imaging.* 2015;25:213–25.
7. Concepcion NDP, Laya BF, Andronikou S, et al. Standardized radiographic interpretation of thoracic tuberculosis in children. *Pediatr Radiol.* 2017;47:1237–48.
8. Sodhi KS, Bhalla AS, Mahomed N, Laya BF. Imaging of thoracic tuberculosis in children: current and future directions. *Pediatr Radiol.* 2017;47:1260–8.
9. Bosch-Marcet J, Serres-Créixams X, Zuasnar-Cotro A, Codina-Puig X, Català-Puigbó M, Simon-Riazuelo JL. Comparison of ultrasound with plain radiography and CT for the detection of mediastinal lymphadenopathy in children with tuberculosis. *Pediatr Radiol.* 2004;34:895–900.
10. Lew WJ, Jung YJ, Song JW, et al. Combined use of QuantiFERON-TB gold assay and chest computed tomography in a tuberculosis outbreak. *Int J Tuberc Lung Dis.* 2009;13:633–9.
11. Veedu PT, Bhalla AS, Vishnubhatla S, et al. Pediatric vs adult pulmonary tuberculosis: a retrospective computed tomography study. *World J Clin Pediatr.* 2013;2:70–6.
12. Mukund A, Khurana R, Bhalla AS, Gupta AK, Kabra SK. CT patterns of nodal disease in pediatric chest tuberculosis. *World J Radiol.* 2011;3:17–23.
13. Kaur R, Jana M. Imaging in chest tuberculosis. In: Bhalla AS, Jana M, editors. *Clinico-Radiological Series: Imaging of Chest Infections*, 1st ed. New Delhi: Jaypee Brothers Medical Publishers; 2018. p. 124–45.
14. Moyes EN. Tuberculoma of the lung. *Thorax.* 1951;6:238–49.
15. Naranje P, Guleria R. Imaging of infections of pleura and chest wall. In: Bhalla AS, Jana M, editors. *Clinico Radiological Series: Imaging of Chest Infections*, 1st ed. New Delhi: Jaypee Brothers Medical Publishers; 2018. p. 385–403.
16. Arora A, Bhalla AS, Jana M, Sharma R. Overview of airway involvement in tuberculosis. *J Med Imaging Radiat Oncol.* 2013;57:576–81.
17. Rizzi EB, Schinina' V, Cristofaro M, et al. Detection of pulmonary tuberculosis: comparing MR imaging with HRCT. *BMC Infect Dis.* 2011;11:243.
18. Manson DE. MR imaging of the chest in children. *Acta Radiol.* 2013;54:1075–85.
19. Baez JC, Ciet P, Mulkern R, Seethamraju RT, Lee EY. Pediatric chest MR imaging: lung and airways. *Magn Reson Imaging Clin N Am.* 2015;23:337–49.
20. Sodhi KS, Khandelwal N, Saxena AK, et al. Rapid lung MRI in children with pulmonary infections: time to change our diagnostic algorithms. *J Magn Reson Imaging.* 2016;43:1196–206.
21. Vorster M, Sathekge MM, Bomanji J. Advances in imaging of tuberculosis: the role of <sup>18</sup>F-FDG PET and PET/CT. *Curr Opin Pulm Med.* 2014;20:287–93.
22. Pelletier-Galarneau M, Martineau P, Zuckier LS, Pham X, Lambert R, Turpin S. <sup>18</sup>F-FDG-PET/CT imaging of thoracic and extrathoracic tuberculosis in children. *Semin Nucl Med.* 2017;47:304–18.
23. Willowson KP, Bailey EA, Bailey DL. A retrospective evaluation of radiation dose associated with low dose FDG protocols in whole-body PET/CT. *Australas Phys Eng Sci Med.* 2012;35:49–53.